- Technical Paper -

SIMULATION OF TENSION BEHAVIOR OF REINFORCED CONCRETE MEMBERS STRENGTHENED WITH CFS BY USING RBSM

Khalid FARAH[*1] and Yasuhiko SATO[*2]

ABSTRACT

This paper presents numerical simulation to the tension behaviour of reinforced concrete (RC) members strengthened with externally bonded Carbon Fiber Sheets (CFS) by using two dimensional Rigid Body Spring Model (RBSM) ([1] and [2]). A non-linear reinforced concrete model strengthened by CFS, with bond-slip models and bond deterioration models to simulate both the steel reinforcement bar–concrete interface and the CFS-concrete interface were applied in the RBSM numerical code. It is reported that the RBSM analysis can represent the experimentally observed phenomena very well.

Keywords: reinforced concrete, strengthened, carbon fiber sheets, RBSM, bond deterioration model

1. INTRODUCTION

Strengthening or retrofitting the reinforced concrete (RC) members by using the externally bonded Carbon Fiber Sheet (CFS) has proven its efficiency to improve the performance of the strengthened element in axial, shear, and bending. In all the application of externally bonded CFS the most critical point is the bond behavior at the CFS-concrete interface (Japan Concrete Institute [3] and Sato et al. [4]). Bond deterioration due to concrete cracking is considered one of the major reasons which lead to debonding or loosing the bond action between concrete and CFS which cause premature failure prior to the theoretical ultimate load. Although there is number of experimental works that was done to investigate the effect of CFS on crack spacing, crack pattern and tension stiffening of reinforced concrete elements in tension (Ueda et al [5]) plus the available numerical models (Sato et al. [6] and Pecce and Ceroni [7]).This phenomena did not fully clarified yet. This study was conducted to provide numerical model to simulate the pure tension behavior of concrete element with internal reinforcement and external CFS. The steel reinforcement-concrete interface and CFS-concrete interface were modeled by using bond-slip models in the un-cracked sections, while in the cracked sections simplified bond deterioration models were applied to simulate the crack effect on bond and the bond deterioration due to concrete cracking.

2. EXPERIMENTAL APPROACH

In this study some specimens that were experimented by Ueda et al [5] will be used as experimental evidence to validate the numerical model. Specimen were concrete prisms with cross section of 150×150 mm with a deformed bar embedded at the center of the cross section and carbon fiber sheets (CFS) externally bonded to their two side surfaces, as shown in Fig.1. The experimental parameter was the CFS ratio (ρ_{CFS}) as shown in Table 1. The width of the CFS was narrower than the prism width where the prism width was 150 mm and CFS width was 120 mm. Strain gauge were mounted on the steel bar at 40 mm spacing and on the top layer of CFS at 20 mm spacing in the test zone of 1200 mm. Contact chips were mounted on the concrete surface at 60 mm spacing to measure the crack widths. Both ends of the prisms were reinforced by steel plate and lateral reinforcement. The Table1 and Fig.1 show the details of all specimens.

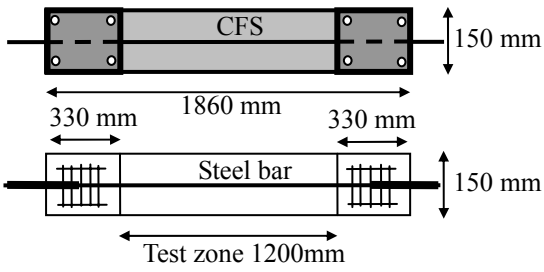

Fig. 1 Specimen layout

All the specimens were pulled statically through a deformed bar embedded in the concrete prism by a hydraulic jack. Strains of the reinforcing bar and CFS as well as concrete crack widths were measured. The local bond stresses were calculated from the measured strains, by using Eq. 1.

$$\tau = \frac{AE\Delta\varepsilon}{A_{bo}\Delta x} \quad (1)$$

Where A and E are cross-sectional area and Young's modulus of the steel bar reinforcement/CFS; A_{bo} is bonding area per unit length; $\triangle\varepsilon$ is the difference in the strain of the steel bar reinforcement/CFS; and $\triangle x$ is the

*1 Ph. D. candidate, Division of Built Environment, Hokkaido University, Msc, JCI Member
*2 Associate Prof., Division of Built Environment, Hokkaido University, Dr.E., JCI Member

difference in the location. The concrete compressive strength was 30 MPa for all of the specimens; the material properties of the deformed bar and CFS are shown in Tables 2 and 3, respectively.

Table 1. Details of experimental specimens

Specimen	Type of reinforcement bar	Cover (mm)	ρ_S	ρ_{CFS}
S-3-0	D19	65.5	1.27	0
S-3-1	D19	65.5	1.27	0.12
S-3-2	D19	65.5	1.27	0.23

Table 2. Material properties of steel reinforcement

Steel bar	Diameter (mm)	E_s (GPa)	ε_y (%)
D19	19.1	170	0.230

Note: E_s=Young's modulus; ε_y=Yielding strain

Table 3. Material properties of carbon fiber sheet

t (mm)	ρ (g/m^2)	F_t (MPa)	E_{CFS} (GPa)	ε_u (%)
0.11	200	3479	230	1.5

Note: t=Thickness; ρ=Fiber Density; F_t=Tensile Strength; E_{CFS}= Young's modulus; ε_u=Fracture strain

3. NUMERICAL APPROACH

The advance design processes require direct understanding of damage evaluation and failure mode plus the loading capacity. So that the numerical model that can predict the fracture condition, crack formation and propagation plus the overall performance is highly required. There are several numerical approaches to simulate the behavior of reinforced concrete members. The finite element method (FEM) was applied to provide the over-all performance of reinforced concrete structure. FEM provides reasonable prediction for loading capacity and formation of cracks but in the same time it is hard to get realistic fracture condition such as crack pattern. The discrete methods have the ability to model the materials discontinuity relative to continuum models like most finite element approaches where the materials are represented as a system of numerous discrete particles. The discrete model has the ability to model the brittle failure mode plus the localization process which accompany the fracture of brittle material.

The rigid body spring model (RBSM) which was first developed by Kawai [1] is one of these discrete methods. RBSM code that was developed by the authors will be used in this study as numerical approach instead of the common FEM because of its simplicity in modeling the different materials discontinuity (concrete, steel reinforcement and CFS) plus it is ability to provide reasonable prediction for loading capacity, crack initiation and propagation and overall performance [2]. RBSM has the ability to describe the localization process which accompanies the fracture in brittle-matrix composite materials like the failure of CFS-concrete interface (debonding).

3.1 Rigid Body Spring Model (RBSM)

The Rigid body spring model (RBSM) represents the continuum material as an assemblage of rigid particle elements interconnected along their boundaries through flexible interface. The interface may be viewed as zero-size springs whose initial properties can be set to approximate the overall elastic properties of the continuum. The response of the spring model provides comprehension of the interaction between particles instead of the internal behavior of each particle based on a continuum mechanics. Each rigid particle has three degree of freedom are defined at the arbitrary point within the particle; two translations and one rotational degree of freedom. The flexible interface between particles (interparticle boundaries) consists of three springs in the normal, tangential and rotations as shown in Fig. 2. Since concrete cracks initiate and propagate along interparticle boundaries, the fracture directions and crack pattern is strongly affected by the mesh design. So that the material will be partition into an assemblage to rigid particles by using random geometry by using Voronoi diagrams to reduce the mesh bias on potential crack directions (Bolander and Saito [2])

3.2 Concrete Models

Fracture initiation and propagation are modeled successfully by introducing fracture criterion of concrete material into spring properties. Fracture criterion in RBSM is not based on a tensorial measure of stresses, but utilizes the average stresses acting normal and tangential to the particle interface.

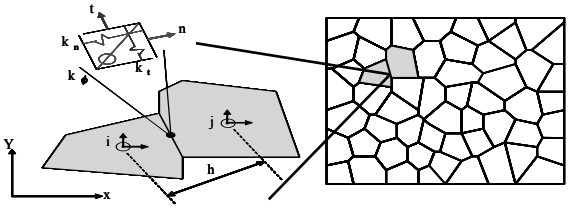

Fig. 2 Rigid Body Spring Model

The criterion is rather simply constructed. That is, uni-axial stress-strain relationships can be introduced into the individual springs. In this study the concrete in compression shows nonlinear behavior up to the compressive strength then after the peak the linear softening branch take place till failure as in Eq. 2.

$$\sigma=\begin{cases} E\varepsilon-\dfrac{E}{2\varepsilon_0}\varepsilon^2 & for \quad \varepsilon\le\varepsilon_0 \\ F_c-\left(\dfrac{F_c-\mu F_c}{\varepsilon_{CU}-\varepsilon_0}\right)(\varepsilon-\varepsilon_0) & for \quad \varepsilon_0<\varepsilon\le\varepsilon_{CU} \\ \mu F_c & for \quad \varepsilon>\varepsilon_{CU} \end{cases} \tag{2}$$

Where: E=modulus of elasticity (MPa), F_c=compressive strength (MPa), ε= compression strain, $\varepsilon_0=2F_c/E$, $\varepsilon_{CU}=4\varepsilon_0$, μ=0.2.

Concrete in tension behaves linearly elastic up to tensile strength then the stress-strain relationship

exhibits strain softening till failure. The softening part depends on the crack width [8] as shown in Eq. 3

$$\frac{\sigma}{F_t}=\left\{1+(C_1\frac{W}{W_C})^3\right\}\exp(-C_2\frac{W}{W_C})-\frac{W}{W_C}(1+C_1^3)\exp(-C_2) \qquad (3)$$

$$W_C=5.14\frac{G_F}{F_t}$$

$$G_F=10(D_{\max})^{1/3}F_c^{1/3}$$

Where: W=crack width (10^{-6}m), σ =tensile stress (MPa), C_1=3, C_2=6.93, W_C= critical crack width where no stress can be transferred (10^{-6}m), G_F= fracture energy (N/mm), D_{max}= maximum size of aggregate (mm).

3.3 Steel reinforcement Model

Each reinforcement bar is modeled by using series of one-dimensional beam elements with axial, shear and flexural rigidities [2]. Two translational and one rotational degree of freedom are defined at each beam element end as shown in Fig. 3. The stress-strain relationship of reinforcement had been used as tri-linear model as shown in Eq 4.

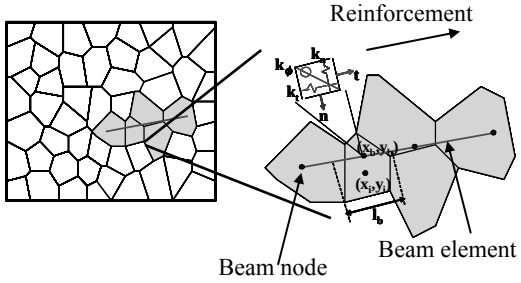

Fig. 3 Continuous reinforcement with zero-size linkage element.

$$\sigma=\begin{cases}E_s\times\varepsilon & \varepsilon<\varepsilon_y\\ E_s\times\varepsilon_y & \varepsilon_y\le\varepsilon<\varepsilon_h\\ E_s\times\varepsilon_y+E_h\times(\varepsilon-\varepsilon_y) & \varepsilon\ge\varepsilon_h\end{cases} \qquad (4)$$

Where; E_s is the elastic modulus of elasticity (MPa), ε is the steel strain, ε_y is the yielding strain, ε_h is the strain when hardening strain starts and E_h is the stiffness when the strain hardening starts.

The bond-slip will be represented by introducing the bond slip relation into the linkage element spring parallel to steel reinforcing bar. The bond slip model proposed by Shima et al [9] and modeled by Eq. 5 will be used.

$$\frac{\tau}{F_c}=\frac{0.73\ (\ln(\ 1+5s\ ))^3}{1+\varepsilon\times10^5} \qquad (5)$$

$$s=1000\ \ S/D$$

Where; τ=bond stress (MPa), S=slip (mm), D=bar diameter (mm), ε=steel strain and F_c=concrete compressive strength (MPa).

3.4 Carbon Fiber Sheet (CFS) Model

For CFS the same beam element that was used for steel reinforcement bar was used. The stress strain relationship was used as linear relationship up to failure. The bond stress-slip-strain model proposed by Sato et al [4] was introduced into the linkage spring parallel to the CFS to simulate the bond slip interaction between CFS and concrete in the un-cracked section.

3.5 Bond Deterioration Model for Steel-Concrete Interface.

When reinforcing bar is tensioned against concrete, splitting conical cracks appear because the ribs of the reinforcing bar press against concrete causing conical diagonal compressive struts. In direction perpendicular to these compressive struts tensile stresses are generated causing these splitting conical cracks. In the vicinity of crack planes, these compressive struts have no concrete to support because of the penetration of conical cracks reaching to the crack planes. So that, concrete spalling takes place causing bond deterioration. The modeling of bond in the cracks locations is important for the post yield behavior because the localization of plastic yielding is initiated from the bond deterioration zone. (Qureshi and Maekawa [10]) in the RC joint model, proposed that the bond stress is decreasing in linear fashion till zero value in distance equal 5D from the crack surface, where D is the bar diameter, and the bond stress drops suddenly to zero at a distance 2.5D from the crack surface due to splitting and crushing of concrete around the bar beside the crack surface as shown in Fig. 4

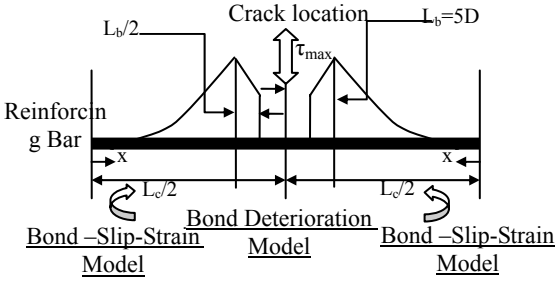

Fig. 4 Bond deterioration close to cracks (Qureshi and Maekawa [10])

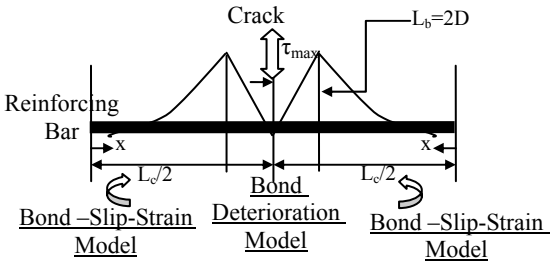

Fig. 5 Proposed simplified bond deterioration model

Salem and Maekawa [11] had modified Qureshi and Maekawa [10] bond deterioration model for small crack spacing where, they proposed that bond deterioration zone is not fixed length (5D) but it depends on the crack spacing. The bond deterioration zone varied from 5D for crack spacing equal 10D to

zero for crack spacing equal 5D or less. In this study simple bond deterioration model proposed as shown in Fig. 5, the bond stress decrease linearly from maximum bond stress to zero in bond deterioration zone equal (2D) this model was proposed to cover both control specimen and strengthened specimens because the crack spacing is changed from (15D) in control specimen to (5D) in strengthened specimen.

3.6 Bond Deterioration Model for CFS-Concrete Interface.

Although there are many studies on bond behavior of continuous fiber sheet, there are very few studies that focus on the deterioration of this bond and what the mechanisms of that deterioration (Sato et al. [6]). Sato et al. [4] proposed that, the bond stress differs for different locations along the bonded length; the maximum bond stress decreases linearly till reaches 50% of the maximum bond stress in length equal 30 mm from the starting point of delamination (point of maximum bond stress) and become constant beyond this point and up to 80mm where the maximum bond stress can be reached again as in Fig. 6. The reason of the variation of maximum bond stress can be explained as. The bonding layer of the surface of concrete fracture when the maximum bond stress is reached and the delamination starts, this fracture induces mechanical damage in the bonding layer surrounding the fracture area, this mechanical damage deteriorated the maximum bond stress and the delamination can take place at values less than the maximum bond stress. Ueda et al [5] proposed that the bond deterioration takes place near the main cracks due to formation of diagonal cracks because of the bond of CFS where once these diagonal cracks appear the delamination start to propagate. Other cause of bond deterioration near the main cracks is reversed slip that was observed once the crack spacing became rather small.

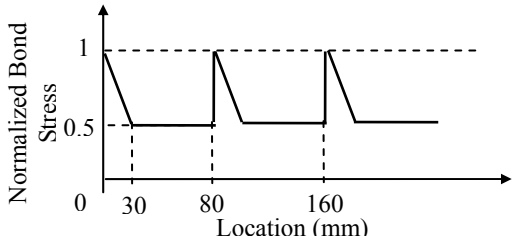

Fig. 6 Bond strength distribution [4]

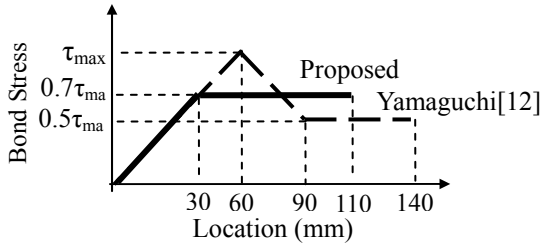

Fig. 7 Bond deterioration models in CFS

Yamaguchi [3] proposed bond deterioration model based on Sato's bond model [4] as shown in Fig.7, where the maximum bond stress is equal to zero at the crack location and increase linearly up to maximum bond stress in distance equal 60 mm from the crack location then decrease linearly up to 50% of the maximum bond stress in distance equal 30 mm where it keeps constant up to distance equal 140 mm from the crack location. The proposed simplified bond deterioration model for CFS-concrete interface is shown in Fig.7, where the maximum bond stress become zero at the crack location and increase linearly in distance equal 30 mm from the crack location up to 70% of the maximum bond stress then it remain constant to this value up to 110 mm from the crack location then after this the normal bond –slip model can be applied. The value of 70% of the maximum bond stress was used because the maximum bond stress in the bond deterioration zone can not be reached due to the mechanical damage of the bonded layer due to cracking which leads to debonding prior to reaching the maximum bond stress. The value of 70% was proposed based on the maximum bond stress variation proposed by Sato et al. [4] as shown in Fig. 6 where the area under this variation curve equal to the area under the proposed bond deterioration model for length equal 80mm.

4. VERIFICATION OF THE NUMERICAL MODEL

4.1 Verification of Bond Deterioration Model for Steel-concrete Interface

To validate the bond deterioration model of steel-concrete interface the numerical analysis for the control specimen (S-3-0) was done with proposed model, the existing model and no bond deterioration model as mentioned in Table 4.

Table 4. Numerical specimens of specimen S-3-0

Experimental. Specimen.	Numerical Specimen	bond deterioration model
S-3-0	RBSM S-3-01	No model
	RBSM S-3-02	Existing model
	RBSM S-3-03	Proposed model

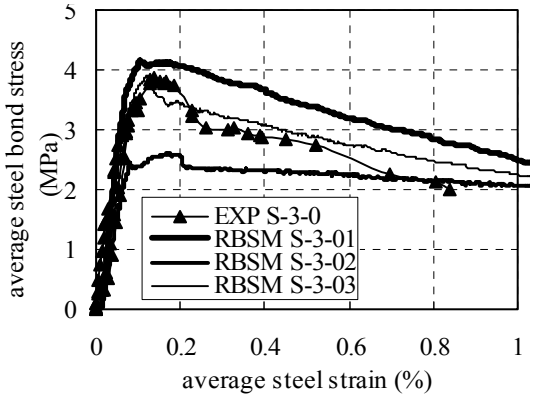

Fig. 8 Average strain- average bond stress in steel reinforcement for specimen S-3-0

Fig. 8 shows the relationship of average steel strain–average bond stress for the control specimen S-3-0. Satisfied agreement between the experimental

results and the numerical results of the proposed bond deterioration model can be found, while the case with no bond deterioration model shows greater average bond stress specially in the softening part where the bond deterioration due to cracks takes effect. The case of the existing bond deterioration model shows smaller average bond stress due to the largest of bond deterioration length (5D).

4.2 Verification of Bond Deterioration Model for CFS-Concrete Interface

To validate the bond deterioration model for CFS-concrete interface the numerical analysis for the specimens in Table 5 was done. The simplified bond deterioration model for steel-concrete interface was used for all the specimens in Table 5.

Table 5. Numerical specimens of specimen S-3-1

Experimental. Specimen	Numerical Specimen	Type of bond deterioration
S-3-1	RBSM S-3-11	No model
	RBSM S-3-12	Existing model
	RBSM S-3-13	Proposed model

Fig. 9 shows the relation of average strain and average bond stress of CFS for different bond deterioration model for CFS-concrete interface the existing bond deterioration model [12] and the proposed model give very good agreement with comparison with the experimental results while the proposed model has the advantage of the simplicity. The analysis with no bond deterioration shows greater average bond stress for CFS which leads to the important of the bond deterioration model of CFS-concrete interface.

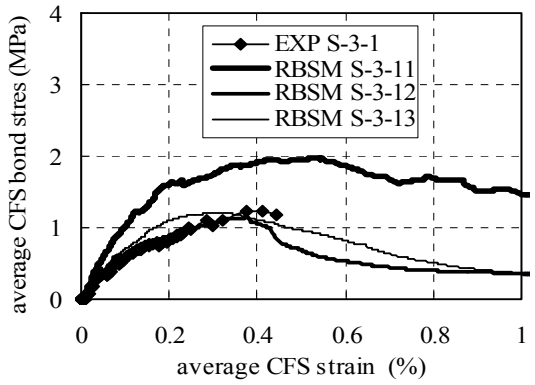

Fig. 9 Average strain- average bond stress in CFS for specimen S-3-1

4.3 Effect of CFS on the Behavior of Reinforced Concrete Member.

Fig. 10 indicates relationships between the average bond stress and the average strain of steel bar reinforcement. The average bond stress was calculated as the average of the local stress in the test zone, while the average strain was calculated as the average of the local measured strains. Fig. 10 clearly shows that the average bond stress in specimen without CFS (specimen S-3-0) is greater than those in specimens with CFS (specimens S-3-1 and S-3-2). This due to, by applying the CFS the crack spacing decreases, the number of cracks increases and the length of deteriorated bond for steel–concrete interface increases then the average bond stress decreases. The same action happens if the CFS stiffness increases. Fig. 10 indicates accepted agreement between the numerical and the experimental results except for specimen (S-3-2) at average strain greater than 0.2% the reason for this poor agreement is under discussion. Relationship between the average CFS strain and average CFS bond stress are given in Fig. 11. CFS with a greater stiffness or more layers indicates greater average bond stress than CFS with a smaller stiffness. Peak average bond stress was observed after the delamination of CFS.

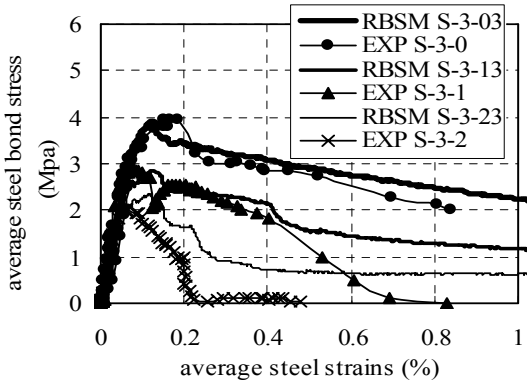

Fig. 10 Average strain- average bond stress in steel reinforcement

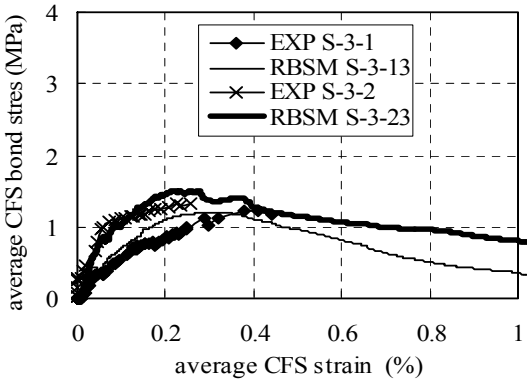

Fig. 11 Average strain- average bond stress in CFS

The average stress-average strain relationship of the steel bar shown in Fig. 12 is compared with the same relationship for the bare bar (steel reinforcement bar without concrete). The results indicate that the yielding stress is smaller than that for the bare bar this due to the fact that the yielding takes place at the cracks intersection, and the strain between cracks are still smaller than the yielding strain at that time. Fig. 12 indicates that a greater CFS ratio makes the relationship closer to that of the bare bar. This is because a greater CFS ratio brings about smaller crack spacing and then smaller bond stress between the steel bar and concrete. Fig. 13 indicates the relationships between the average strain and the average crack width. Fig. 13 indicates

that the average crack width in specimens with CFS (S-3-1 and S-3-2) became smaller than those in specimen without CFS (S-3-0). This fact is believed to be due to smaller crack spacing in the case with CFS, where the average crack spacing in specimen without CFS was 300 mm and the average crack spacing in specimen with one layer and two layers of CFS was 170 mm and 160mm respectively. A similar tendency can be seen in the previous studies (Ueda et al [5]).

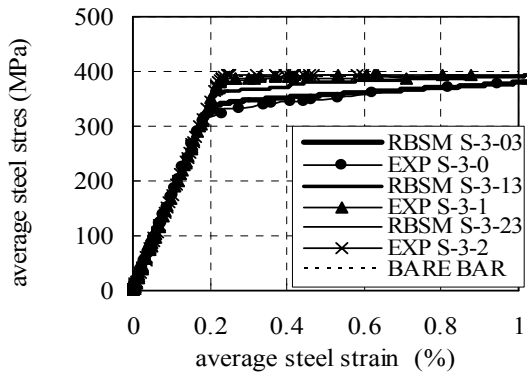

Fig. 12 Average steel strain- average steel stress

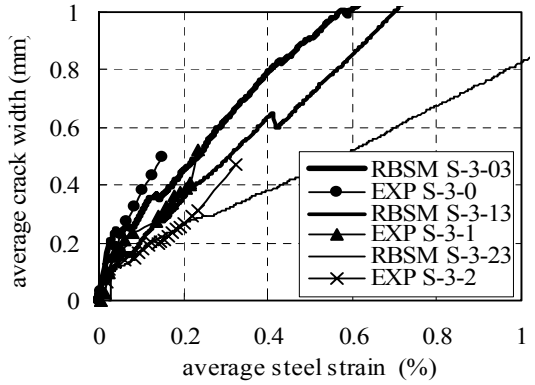

Fig. 13 Average steel strain- average crack width

5. CONCLUSIONS

Based on the RBSM numerical code, numerical model was presented to simulate the behavior of reinforced concrete member strengthened with CFS. A non-linear reinforced concrete model strengthened by CFS, with bond-slip models to simulate the steel reinforcement bar-concrete interface and CFS-concrete interface in the un-cracked sections plus simplified bond deterioration models in the cracked sections. This study had proved the validity of the proposed simplified bond deterioration models with comparing to the existing models. The applicability of the model was proved by comparing the numerical results with the experimental one. Satisfied agreement between the experimental and numerical results was presented. From the numerical results CFS shows significant effect on the average stress and average bond stress of steel reinforcement bar and average crack width.

ACKNOWLEDGEMENT

The first author acknowledges the financially supports of Ministry of Higher Education, Arab Republic of Egypt to his scholarship.

REFERENCES

[1] Kawai, T., "New Discrete Model and Their Application to Seismic Response Analysis of Structure", J. of Nuclear Engineering and Design, No. 48, pp. 207-229, 1987.

[2] Bolander, j. E. and Saito, S., "Fracture Analysis using Spring Network Models with Random Geometry", J. of Engineering Fracture Mechanics No. 61, pp. 569-591, 1998.

[3] Japan Concrete Institute (JCI), "Technical Reports on Continuous Fiber Reinforced Concrete", TC952 on continuous fiber reinforced Concrete, Tokyo.

[4] Sato, Y., Asano, Y., and Ueda, T., "Fundamental Study on Bond mechanism of Carbon Fiber Sheet", Concrete library Int., 37, pp, 97-115, 2001.

[5] Ueda, T., Yamaguchi, R., Shoji, K., and Sato, Y., "Study on Behavior in Tension of Reinforced Concrete Members Strengthened by Carbon Fiber Sheet", J., of Compos., for Cons., ASCE, 6(3), pp. 168-174, 2002.

[6] Sato, Y., Ueda, T., and Shoji, K., Tension Stiffening Effect of Reinforced Concrete Members Strengthened by Carbon Fiber Sheet", Proc., of Int., Symp., Bond in Concrete-from Research to Standards, Publishing Company of Budapest University of Technology and Economics, Budapest, Hungary, pp. 606-613, 2002.

[7] Pecce, M., and Ceroni, F., "Modeling of Tension-Stiffening Behavior of Reinforced Concrete Ties Strengthened with Fiber Reinforced Plastic Sheets" J. of Comp., for Const., ASCE, Vol. 8, No. 6, pp. 510-518, 2004.

[8] Hordijk, D., A., "Local Approach to Fatigue of Concrete", Thesis, Technical University of Delft, pp. 66-77, 1991.

[9] Shima, H., Chou, L. and Okamura, H., "Micro and Macro Models for Bond in Reinforced Concrete", J., of The Faculty of Engineering, Tokyo University Vol. XXXIX, No.2, pp. 133-197, 1987.

[10] Quraeshi, J., and Maekawa, k. "Computational Model for Steel bar Embedded in Concrete Under Combined Axial Pullout and Transverse Shear Displacement", Proc. of JCI, Vol., 15, No., 2, pp. 1249-1254, 1993.

[11] Salem, H., and Maekawa, K., "Spatially Averaged Tensile Mechanics for Cracked Concrete and Reinforcement under Highly Inelastic Range", J., Materials, Conc. Struct. Pavement, JSCE, No. 613, Vol. 42, pp. 277-293, 1999.

[12] Yamaguchi, R., "A study on Uni-axial Tension Behavior of RC Members Strengthened with Carbon Fiber Sheet", Master Dissertation, Hokkaido University, 2000.